

Testing that a Local Optimum of the Likelihood is Globally Optimum using Reparameterized Embeddings

Applications to Wavefront Sensing

Joel W. LeBlanc^{1,2} · Brian J. Thelen^{1,2} · Alfred O. Hero¹

Received: date / Accepted: date

Abstract Many mathematical imaging problems are posed as non-convex optimization problems. When numerically tractable global optimization procedures are not available, one is often interested in testing ex post facto whether or not a locally convergent algorithm has found the globally optimal solution. When the problem is formulated in terms of maximizing the likelihood function of using a statistical model, a local test of global optimality can be constructed. In this paper, we develop such a test, based on a global maximum validation function proposed by Biernacki, under the assumption that the statistical distribution is in the generalized location family, a condition often satisfied in inverse problems. In addition, a new reparameterization and embedding is presented that exploits knowledge about the forward operator to improve the global maximum validation function. It is shown that the reparameterized embedding can be gainfully applied to a physically-motivated joint-inverse problem arising in camera-blur estimation. Improved accuracy and reduced computation are demonstrated for the proposed global maximum testing method.

Keywords inverse problems · parameter estimation · maximum likelihood · global optimization · local maxima

PACS 42.30.-d · 02.30.Zz · 02.70.Rr · 02.60.Cb

✉ Joel W. LeBlanc^{1,2}
E-mail: jwleblan@umich.edu

¹ University of Michigan
Ann Arbor, Michigan, 48109, USA

² Michigan Tech Research Institute
Ann Arbor, Michigan, 48105, USA

1 Introduction

Mathematical imaging problems are often formulated as non-convex energy minimization problems that imposes desirable properties on the global minimum, e.g., corresponding to a denoised, deblurred, or segmented image. Much of the work of Mila Nikolova addressed the problem of local and global minima. As stated succinctly in one of her early papers: “The resultant ... energy generally exhibits numerous local minima. Calculating its local minimum, placed in the vicinity of the maximum likelihood estimate, is inexpensive but inadequate” [25]. Study of local and global minima was a recurring theme in her work, in which she addressed the nature of objective functions associated with non-convex probabilistic models, i.e., maximum likelihood (ML) and maximum a posteriori (MAP) [24], [28], [25], [27], [3], [26], as well as non-linear least squares [13], [14]. Some of the optimization algorithms she introduced were only shown to converge to one of several possible local minima. For such algorithms, an important question is whether or not an observed convergent limit is, in fact, the global minimum. Searching for, and identifying, the global minimum is the problem that we address in this paper.

We consider this problem in the general setting of maximum likelihood parameter estimation from multiple samples coming from a probability distribution that belongs to a parametric family. The conceptual simplicity and tractability of the Maximum Likelihood (ML) principle, along with its theoretical optimality properties, has made ML approaches prevalent in many fields. Yet, questions surrounding its practical application remain open. The pioneering statistician Sir Ronald Fisher [15] was an early advocate of the ML approach and is generally credited with its development, although similar concepts predate Fisher’s work. Stigler [35] provides a

historical account of the theory’s maturation throughout the nineteenth and twentieth centuries. Asymptotic (large sample) characterization of local vs. global optima of the likelihood function was established by Le Cam (c.f. [20], ch. 6) using central limit theory, but can be challenging to apply in practice. As the sample size increases, it has long been known that, under mild smoothness conditions, all statistically consistent stationary points of the likelihood function converge with probability one to the global maximum [12, 37]. The natural question then becomes: when there exist multiple stationary points, and the number of samples is finite, how can one identify the globally optimal one?

There exist general-purpose algorithms to address this question, e.g., simulated annealing and genetic algorithms. These algorithms, however, are rarely applied to high-dimensional problems because of high computational demands [4, 5, 33]. Stationary points of the gradient of the likelihood function can be readily found using iterative root-finding methods such as Quasi-Newton gradient descent [29]. Once a stationary point is found, it would be useful to have access to a simple test to determine whether or not it is global optimal without knowing the maximum value of the likelihood function. Several such tests have been proposed for this purpose [7], [8]. In this paper, the focus is on testing local maxima of the likelihood function in the context of high dimensional inverse-problems arising in signal processing and imaging.

Specifically, this paper makes the following contributions. Starting with the global maximum validation function introduced by Biernacki [7], we demonstrate that its mean is always less than or equal to zero when the likelihood function belongs to a generalized location family of distributions: distributions parameterized by a shift in location. This property provides the impetus for constructing a one-sided variant of the test. This generalized location family includes both linear and non-linear inverse-problems. Finally, we introduce a new approach for constructing application-specific tests based on reparameterized embeddings and provide a means of identifying useful candidate embeddings. This approach is shown to have performance advantages, and its computational efficacy is demonstrated on a physically motivated inverse-imaging problem [21].

The remainder of the paper is organized as follows. Section 2 describes the general problem and introduces a specific example, which is used throughout the work to demonstrate the key concepts. Section 3 describes Biernacki’s two-sided test for convergence to a local minimum, introduces a new one-sided variant, and describes a new test based on reparameterized embeddings. The performance of each of these tests is compared numeri-

cally. Finally, Section 4 describes an application of the proposed testing approach to image blur estimation.

2 Problem Description

2.1 Background

The problem setting is the following. Assume the data are in the form of a matrix $\mathbf{d} = [\mathbf{d}_1, \dots, \mathbf{d}_n] \in \mathbb{R}^{m \times n}$ where the columns are independent and identically distributed (i.i.d.) realizations of an m -dimensional random vector \mathbf{D}_1 having a parametric density $f(\mathbf{d}_1; \boldsymbol{\theta})$. The probability distribution $f(\mathbf{d}, \boldsymbol{\theta}) = \prod_{i=1}^n f(\mathbf{d}_i, \boldsymbol{\theta})$ of $\mathbf{D} = [\mathbf{D}_1, \dots, \mathbf{D}_n]$ is a known function of \mathbf{d} and $\boldsymbol{\theta}$ and is assumed to be in a parametric family $\{f(\mathbf{d}; \boldsymbol{\theta}) : \mathbf{d} \in \mathcal{D}, \boldsymbol{\theta} \in \Theta\}$. Here the vector of parameters $\boldsymbol{\theta}$ is unknown, taking values in a parameter space Θ , an open subset of \mathbb{R}^p , and the matrix of measurements \mathbf{d} takes values in a sample space $\mathcal{D} \subset \mathbb{R}^{m \times n}$. We define $\boldsymbol{\theta}_0$ to be a fixed value, called the true value, of the parameter vector. For any mean square integrable function X of \mathbf{D} we define the statistical expectation $E_{\boldsymbol{\theta}_0}[X(\mathbf{D})] = \int X(\mathbf{d})f(\mathbf{d}; \boldsymbol{\theta}_0) d\mu(\mathbf{d})$, where $d\mu(\mathbf{d})$ indicates integration with respect to the Lebesgue measure on \mathbb{R}^m . As the columns of the measurement matrix \mathbf{d} are i.i.d. realizations, the log-likelihood function is

$$\ell(\mathbf{d}; \boldsymbol{\theta}) = \frac{1}{n} \sum_{k=1}^n \ln f(\mathbf{d}_k; \boldsymbol{\theta}) \quad (1)$$

The associated maximum likelihood estimator (MLE) $\hat{\boldsymbol{\theta}} : \mathcal{D} \rightarrow \Theta$ is defined as the global minimum

$$\hat{\boldsymbol{\theta}}_{\text{Global}} = \arg \min_{\boldsymbol{\theta} \in \Theta} -\ell(\mathbf{d}; \boldsymbol{\theta}). \quad (2)$$

An estimator $\hat{\boldsymbol{\theta}}$ is said to be consistent (statistically consistent in norm) when $\lim_{n \rightarrow \infty} E_{\boldsymbol{\theta}_0}[\|\hat{\boldsymbol{\theta}} - \boldsymbol{\theta}_0\|^2] \rightarrow 0$. We will assume that f is continuously differentiable in $\boldsymbol{\theta}$ for all \mathbf{d} , and define the score function as $\mathbf{s}(\mathbf{d}, \boldsymbol{\theta}) = \nabla_{\boldsymbol{\theta}} \ell(\mathbf{d}, \boldsymbol{\theta})$. The Fisher information matrix $\mathbf{I}(\boldsymbol{\theta}_0) = E_{\boldsymbol{\theta}_0}[\mathbf{s}(\mathbf{D}, \boldsymbol{\theta}_0) \mathbf{s}(\mathbf{D}, \boldsymbol{\theta}_0)^T]$ is assumed to exist and be invertible, and the notation “ \xrightarrow{P} ” and “ \xrightarrow{D} ” will be used to describe convergence in probability and distribution respectively.

For the problem addressed in this paper, the global minimum of the negative log-likelihood is unknown and only a local minimum $\hat{\boldsymbol{\theta}}$ is available, which is not necessarily equal to $\hat{\boldsymbol{\theta}}_{\text{Global}}$. For example, the local minimum could be the limit of a convergent gradient descent algorithm. Given $\hat{\boldsymbol{\theta}}$, the local minimum testing problem is to decide between the two hypotheses

$$H_0 : \hat{\boldsymbol{\theta}} = \hat{\boldsymbol{\theta}}_{\text{Global}} \quad \text{vs.} \quad H_1 : \hat{\boldsymbol{\theta}} \neq \hat{\boldsymbol{\theta}}_{\text{Global}}. \quad (3)$$

A test between H_0 and H_1 is defined as a binary valued function $\phi : \mathcal{D} \rightarrow \{0, 1\}$ that maps the data \mathbf{d} to 0 or 1, indicating the decision H_0 or H_1 , respectively. The accuracy of a test is measured by its probability of false alarm $\text{PFA} = E_{\theta_0}[\phi|H_0]$ and its probability of detection $\text{PD} = E_{\theta_0}[\phi|H_1]$. If for two tests ϕ_1 and ϕ_2 having identical PFA, PD of ϕ_1 is greater than PD of ϕ_2 , then ϕ_1 is said to be more powerful than ϕ_2 .

Many approaches to the general hypothesis testing problem (3) have been studied over the years. Blatt and Hero [8] presented a historical context, which is summarized here. The likelihood ratio test [39], Wald test [36], and Rao score test [31] are asymptotically equivalent tests as the number n of samples approaches infinity. The likelihood ratio and Wald tests require the distribution under H_0 to be known, which for (3) requires knowledge of the true parameter. On the other hand, the Rao score test, later independently discovered and popularized under the name Lagrange multiplier test [34], can be implemented when the true parameter is unknown. Rao's test measures the Euclidean norm of the score function weighted by the inverse Fisher information evaluated at a local maximum $\xi_R = \frac{1}{p} \mathbf{s}(\mathbf{d}, \hat{\boldsymbol{\theta}})^T \mathbf{I}^{-1}(\hat{\boldsymbol{\theta}}) \mathbf{s}(\mathbf{d}, \hat{\boldsymbol{\theta}})$. Gan and Jiang [16] propose a similar test for consistency of a stationary point of the log-likelihood based on White's information test [38]. White's original work was concerned with testing for model misspecification under the assumption that the global maximum of the likelihood function had been located, and Gan uses the same test statistic but in the converse situation.

The Rao test may be used to test for consistency of a local maximum of the log-likelihood function. Unfortunately, Monte Carlo experiments indicate that this test may not be very powerful even in the univariate setting [16, 7]. Biernacki [7] suggested an improved test for the consistency of a stationary point following ideas presented by Cox [10, 11]. Biernacki's test uses a bootstrap estimate to directly compare the observed value of the locally maximized log-likelihood to its statistical expectation. Both the Rao score and the Biernacki tests fall under the more general M-testing framework described by Blatt and Hero [8] where additional types of tests of local maxima are proposed.

2.2 A Simple Motivating Example

To illustrate the testing of local maxima of the log-likelihood we consider the following simple statistical inverse problem. Let \mathbf{d} be data measured from a forward model with mean response $\boldsymbol{\mu}(\theta)$ and i.i.d. additive

Gaussian noise $\boldsymbol{\varepsilon}$ of variance σ^2 :

$$\mathbf{d} = \boldsymbol{\mu}(\theta) + \boldsymbol{\varepsilon} \quad \text{s.t.} \quad \boldsymbol{\varepsilon} \sim \mathcal{N}(\mathbf{0}, \sigma^2 \mathbf{I}_{100 \times 100}). \quad (4)$$

The unknown true value of $\boldsymbol{\mu}(\theta_0)$ is a vector of time samples of a sinusoidal signal

$$\boldsymbol{\mu}(\theta_0) = \sin(\theta_0 \mathbf{x}), \quad \theta_0 = 3\pi \quad (5)$$

$$\mathbf{x} = \frac{1}{99} [0, 1, \dots, 99]^T. \quad (6)$$

Suppose it is known *a priori* that $\boldsymbol{\mu}$ is in the signal class $\mathcal{C} = \{\boldsymbol{\mu} : \boldsymbol{\mu} = \sin(\theta \mathbf{x}), \theta \in [0, 4\pi]\}$. The maximum likelihood estimator is then the solution of the constrained optimization problem

$$\hat{\boldsymbol{\theta}}_{\text{Global}} \stackrel{\text{def}}{=} \arg \min_{\theta \in [0, 4\pi]} \|\boldsymbol{\mu}(\theta) - \mathbf{d}\|^2. \quad (7)$$

This one-dimensional parametric model typically generates multiple local minima of the objective function. Figure 1(a) shows two of these local minima for the case that the noise variance σ^2 is zero. The solid curve in Figure 1(a) is the global minimum, which is the true signal, and the dashed curve is another local minimum. This figure also shows the corresponding data observations \mathbf{d} for realizations of these two signals when the noise variance is $\sigma^2 = 1$. The perceptual similarity between these two realizations illustrates the potential difficulty of distinguishing a sub-optimal local minimum from the global minimum. This situation is a stripped down version of the more difficult situation commonly found in inverse-imaging problems (c.f. [21] Section 3c).

3 Tests for Local Optima

In the hypothesis testing problem described by (3), the null-hypothesis H_0 is that the discovered local minimum $\hat{\boldsymbol{\theta}}$ of the log-likelihood is a global minimum. It is important to note that a failure to reject the null hypothesis is not a positive statement about the global optimality of $\hat{\boldsymbol{\theta}}$. Instead, when a test accepts H_0 , all that can be said is that it does not rule out the point as a local minimum with sufficient statistical certainty.

3.1 A Two-Sided Test

To test whether a local maximum of the likelihood function is in fact the global maximum the key is to define a suitable *global maximum validation function* whose statistical distribution changes depending on whether the local minimum $\hat{\boldsymbol{\theta}}$ is global or not [8]. Define the validation function $\varphi(\mathbf{d}, \hat{\boldsymbol{\theta}}) \stackrel{\text{def}}{=} \ell(\mathbf{d}; \hat{\boldsymbol{\theta}}) - m(\hat{\boldsymbol{\theta}}, \hat{\boldsymbol{\theta}})$, where $m : \mathbb{R}^p \times \mathbb{R}^p \rightarrow \mathbb{R}$ is the mean function $m(\boldsymbol{\theta}, \tilde{\boldsymbol{\theta}}) =$

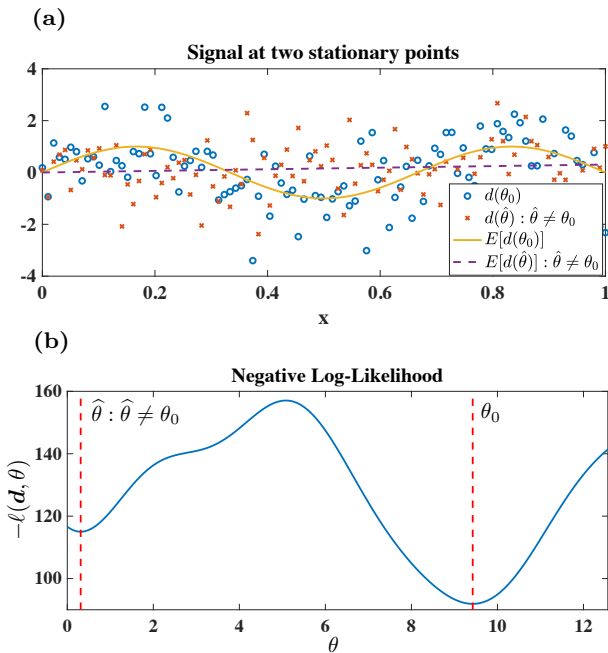


Fig. 1: (a) The measured data plotted with a noise variance is $\sigma^2 = 1$. The true signal (solid) achieving global the minimum and signal (dashed) achieving a sub-optimal local minimum of the likelihood function (7) are also plotted when the noise variance σ^2 equals zero. (b) The negative log-likelihood plotted as a function of θ .

$E_{\theta}[\ell(\mathbf{D}; \tilde{\theta})]$. This is the statistical expectation under the distribution $f(\mathbf{d}; \theta)$ of the log-likelihood function $\ell(\mathbf{D}, \theta)$ evaluated at $\theta = \tilde{\theta}$. Assuming that the global maximum $\hat{\theta}_{\text{Global}}$ is near the true value θ_0 , under the null hypothesis H_0 we have $\hat{\theta} = \hat{\theta}_{\text{Global}}$, and the distribution of $\varphi(\mathbf{D}, \hat{\theta})$ will have approximately zero mean. On the other hand, under the alternative hypothesis H_1 that $\hat{\theta}$ is a non-global local maximum the mean of the distribution of $\varphi(\mathbf{D}, \hat{\theta})$ will shift away from zero. This is the key motivation for using the validation function for testing for a global maximum.

For an i.i.d. data sample $\mathbf{D}_1, \dots, \mathbf{D}_n$ Biernacki established the asymptotic result ([7], Theorem 2) that under H_0 :

$$\frac{1}{\sqrt{n}} \sum_{k=1}^n \varphi(\mathbf{D}_k, \hat{\theta}) \xrightarrow{D} \mathcal{N}(0, \text{Var}_{\theta_0}[\ell(\mathbf{D}_1, \theta_0)]), \quad (8)$$

where $\text{Var}[\ell(\mathbf{D}_1, \theta_0)]$ is the variance of the log-likelihood function for a single data sample ($n = 1$). Recalling the definition of the random data matrix $\mathbf{D} = \{\mathbf{D}_1, \dots, \mathbf{D}_n\}$, this Gaussian limit motivates us to define the hypothesis

test

$$\frac{(\ell(\mathbf{D}; \hat{\theta}) - m(\hat{\theta}, \hat{\theta}))^2}{v(\hat{\theta})} \underset{H_0}{\overset{H_1}{\geq}} \eta, \quad (9)$$

where the function $v: \mathbb{R}^p \rightarrow \mathbb{R}$ is the variance $v(\theta) = \text{Var}_{\theta}[\ell(\mathbf{D}; \theta)]$ under the distribution $f(\mathbf{d}, \theta)$ of the log-likelihood evaluated at θ , and η is a threshold selected to fix the false alarm probability equal to a suitably small number $\alpha \in [0, 1]$. Under local asymptotically normal (LAN) conditions on the likelihood function [22] $\hat{\theta} \xrightarrow{P} \theta_0$ (a.s.) and the test statistic on the left hand side of (9) has an approximately Chi-Square distribution under H_0 . Hence η can be selected as the $1 - \alpha$ quantile of the Chi-square distribution. Biernacki implemented this test by approximating the mean $E_{\theta_0}[\ell(\mathbf{D}; \theta_0)]$ and the variance $\text{Var}[\ell(\mathbf{D}; \theta_0)]$ using a parametric bootstrap estimator.

The test (9) is called a two-sided test because the condition when the null hypothesis is accepted can be equivalently be expressed as

$$-\sqrt{\eta v(\hat{\theta})} \leq \varphi(\mathbf{D}, \hat{\theta}) \leq \sqrt{\eta v(\hat{\theta})}.$$

This is thus a test for which, as compared to the global minimum $\hat{\theta}_{\text{Global}}$, a sub-optimal local minimum $\hat{\theta}$ will cause the test function to undergo a shift in mean, where the shift could either be in a positive or a negative direction.

3.2 A One-Sided Test

If it were known *a priori* that a sub-optimal local minimum causes a negative shift in the mean of the global maximum validation function $\varphi(\mathbf{D}, \hat{\theta})$ a one-sided test would be advantageous over a two-sided test. More specifically, a one-sided test would be expected to have higher power than the two-sided test (9) when for all $\hat{\theta} \neq \theta_0$,

$$m(\hat{\theta}, \hat{\theta}) \geq m(\theta_0, \hat{\theta}), \quad (10)$$

where, as above, $m(\theta, \hat{\theta})$ is the mean function $E_{\theta}[\ell(\mathbf{D}; \hat{\theta})]$. When this condition is satisfied the two-sided test (9) can be replaced by the one-sided test

$$\frac{\ell(\mathbf{D}; \hat{\theta}) - m(\hat{\theta}, \hat{\theta})}{\sqrt{v(\hat{\theta})}} \underset{H_1}{\overset{H_0}{\geq}} \eta_1. \quad (11)$$

The condition (10) is satisfied for many imaging and inverse problems. For example, consider the case where θ is a clean image that one wishes to recover

from samples of \mathbf{D} , the output of an imaging sensor with known point spread function (forward operator) in additive correlated noise. When the point-spread function (PSF) and the covariance are known, we will show that this model always satisfies the inequality (10), and the one-sided test might be expected to lead to a better test for local minima. Define $\boldsymbol{\theta}_0 \in \mathbb{R}^p$ as the vectorized true image to be recovered and $\mathbf{D} \in \mathbb{R}^q$ as the random vectorized image acquired from the camera, which obeys the model:

$$\mathbf{D} = \mathbf{H}\boldsymbol{\theta}_0 + \varepsilon \quad \text{s.t.} \quad \varepsilon \sim \mathcal{N}(\mathbf{0}, \boldsymbol{\Sigma}), \quad (12)$$

where \mathbf{H} is a $q \times p$ matrix representing the forward operator and $\boldsymbol{\Sigma}$ is the $q \times q$ camera noise covariance matrix.

To show that (10) holds in this case, start with the log-likelihood function for the above model

$$\begin{aligned} \ell(\mathbf{D}; \boldsymbol{\theta}) = & -\frac{1}{2} (\mathbf{H}(\boldsymbol{\theta}_0 - \boldsymbol{\theta}) + \varepsilon)^T \boldsymbol{\Sigma}^{-1} (\mathbf{H}(\boldsymbol{\theta}_0 - \boldsymbol{\theta}) + \varepsilon) \\ & - \frac{1}{2} \ln(\det \boldsymbol{\Sigma}) - \frac{q}{2} \ln(2\pi). \end{aligned} \quad (13)$$

For any value of $\boldsymbol{\theta}$, (13) is a quadratic form in ε that is distributed non-central chi-squared with non-centrality parameter

$$\lambda = (\boldsymbol{\theta}_0 - \boldsymbol{\theta})^T \mathbf{H}^T \boldsymbol{\Sigma}^{-1} \mathbf{H} (\boldsymbol{\theta}_0 - \boldsymbol{\theta}). \quad (14)$$

The moment properties of the non-central chi-square distribution [18] thus specify the statistical expectation of the log-likelihood function (13) :

$$\mathbb{E}_{\boldsymbol{\theta}_0}[\ell(\mathbf{D}; \boldsymbol{\theta})] = -\frac{1}{2} (q + \lambda) - \frac{1}{2} \ln(\det \boldsymbol{\Sigma}) - \frac{q}{2} \ln(2\pi). \quad (15)$$

The difference $\mathbb{E}_{\boldsymbol{\theta}}[\ell(\mathbf{D}; \boldsymbol{\theta})] - \mathbb{E}_{\boldsymbol{\theta}_0}[\ell(\mathbf{D}; \boldsymbol{\theta})] = \lambda/2$, is non-negative, establishing (10) holds as claimed. For this example, the unconstrained maximum likelihood estimator of $\boldsymbol{\theta}$ is a solution to a convex optimization problem, which is strictly convex when \mathbf{H} is full column-rank, and thus there will be no sub-optimal isolated local minima of (2). As our simple example in Figure 1 illustrated, additional constraints can give rise to local minima.

The condition (10) is satisfied for a more general class of camera models where the probability distribution of the data is in the generalized location family.

Definition 1 Let $f(\mathbf{d}; \boldsymbol{\theta})$ be a distribution defined on $\mathbf{d} \in \mathbb{R}^m$ parameterized by $\boldsymbol{\theta} \in \Theta \subset \mathbb{R}^p$. The distribution belongs to the *generalized location family* of distributions if there exists a function $\mathbf{g} : \mathbb{R}^p \rightarrow \mathbb{R}^m$ such that $f(\mathbf{d}; \boldsymbol{\theta}) = f(\mathbf{d} - \mathbf{g}(\boldsymbol{\theta}))$ for all $\boldsymbol{\theta} \in \Theta$ and all $\mathbf{x} \in \mathbb{R}^m$.

Any camera model of the form $\mathbf{D}_k = \boldsymbol{\mu}(\boldsymbol{\theta}_0) + \boldsymbol{\varepsilon}_k$, $k = 1, \dots, n$ where $\boldsymbol{\mu}(\cdot)$ is a possibly non-linear function and $\boldsymbol{\varepsilon}_k$ is i.i.d. but possibly non-Gaussian noise, will have a distribution that is in the generalized location family.

Theorem 1 Let $\mathbf{D}_1, \dots, \mathbf{D}_n$ be an i.i.d. sample and assume that \mathbf{D}_1 has distribution $f(\mathbf{d}_1; \boldsymbol{\theta})$ belonging to a generalized location family. Then the inequality (10) holds.

Proof The proof of the Theorem proceeds in two parts. The first part establishes that, for any parameters $\boldsymbol{\theta}$ and $\boldsymbol{\theta}_0$, $m(\boldsymbol{\theta}_0, \boldsymbol{\theta}_0) \geq m(\boldsymbol{\theta}_0, \boldsymbol{\theta})$. The second part establishes that, for $f(\mathbf{d}; \boldsymbol{\theta})$ in a generalized location family, $m(\boldsymbol{\theta}_0, \boldsymbol{\theta}_0) = m(\boldsymbol{\theta}, \boldsymbol{\theta})$. Putting these two parts together implies

$$m(\boldsymbol{\theta}, \boldsymbol{\theta}) \geq m(\boldsymbol{\theta}_0, \boldsymbol{\theta}).$$

The theorem then follows upon specialization of this inequality to $\boldsymbol{\theta} = \hat{\boldsymbol{\theta}}$.

We recall the integral form for the mean function

$$\begin{aligned} m(\boldsymbol{\theta}, \tilde{\boldsymbol{\theta}}) &= \mathbb{E}_{\boldsymbol{\theta}}[\log f(\mathbf{D}; \tilde{\boldsymbol{\theta}})] \\ &= \int f(\mathbf{d}; \boldsymbol{\theta}) \log f(\mathbf{d}; \tilde{\boldsymbol{\theta}}) d\mu(\mathbf{d}), \end{aligned} \quad (16)$$

and the identity $\mathbb{E}_{\boldsymbol{\theta}}[\log f(\mathbf{D}; \tilde{\boldsymbol{\theta}})] = n\mathbb{E}_{\boldsymbol{\theta}}[\log f(\mathbf{D}_1; \tilde{\boldsymbol{\theta}})]$, which follows from the i.i.d. assumption.

The claim for the first part of the proof follows from the non-negativity property of the Kullback-Liebler divergence, a well known result in statistics and information theory [19]. For completeness, we give a self contained proof. Start with the expression:

$$m(\boldsymbol{\theta}_0, \boldsymbol{\theta}_0) - m(\boldsymbol{\theta}_0, \boldsymbol{\theta}) = - \int f(\mathbf{d}; \boldsymbol{\theta}_0) \log \frac{f(\mathbf{d}; \boldsymbol{\theta})}{f(\mathbf{d}; \boldsymbol{\theta}_0)} d\mu(\mathbf{d}) \quad (17)$$

Now, using the elementary inequality $\log(u) \leq 1 - u$ and the fact that $\int f(\mathbf{d}; \boldsymbol{\theta}) d\mu(\mathbf{d}) = 1$ for all $\boldsymbol{\theta}$, the right hand side of (17) is non-negative. Therefore, using the definition (16), this establishes the claim

$$\mathbb{E}_{\boldsymbol{\theta}_0}[\log f(\mathbf{D}; \boldsymbol{\theta}_0)] \geq \mathbb{E}_{\boldsymbol{\theta}_0}[\log f(\mathbf{D}; \boldsymbol{\theta})].$$

The claim for the second part of the proof is a direct result of $f(\mathbf{d}; \boldsymbol{\theta})$ being in the generalized location family. Specifically,

$$\begin{aligned} m(\boldsymbol{\theta}_0, \boldsymbol{\theta}_0) &= \int f(\mathbf{d}; \boldsymbol{\theta}_0) \log f(\mathbf{d}; \tilde{\boldsymbol{\theta}}_0) d\mu(\mathbf{d}) \\ &= n \int f(\mathbf{d}_1 - \mathbf{g}(\boldsymbol{\theta}_0)) \log f(\mathbf{d}_1 - \mathbf{g}(\boldsymbol{\theta}_0)) d\mu(\mathbf{d}_1) \\ &= n \int f(\tilde{\mathbf{d}}_1 - \mathbf{g}(\boldsymbol{\theta})) \log f(\tilde{\mathbf{d}}_1 - \mathbf{g}(\boldsymbol{\theta})) d\mu(\tilde{\mathbf{d}}_1) \\ &= m(\boldsymbol{\theta}, \boldsymbol{\theta}) \end{aligned}$$

where the second equality comes from the generalized location family definition and the third equality follows from making the change of variable of integration $\tilde{\mathbf{d}}_1 = \mathbf{d}_1 + (g(\boldsymbol{\theta}_0) - g(\boldsymbol{\theta}))$.

This establishes the Theorem. \square

We return to the simple example presented in Section 2.2 to illustrate that the one-sided test (11) gives significant improvement in performance relative to the two-sided test (9) when the distribution $f(\mathbf{d}; \boldsymbol{\theta})$ is in the generalized location family. Figure 2 shows the receiver operating characteristic (ROC) curves for both tests. The ROC of the one-sided test is uniformly better than the two-sided test since it achieves higher power (PD) for any level of false alarm (PFA). This example illustrates how one can exploit knowledge about the nature of the data model to implement a better local minimum test. In the next section, we show how additional improvements in performance can be achieved by exploiting application-specific information, for example, knowledge of the forward operator \mathbf{H} of an inverse problem.

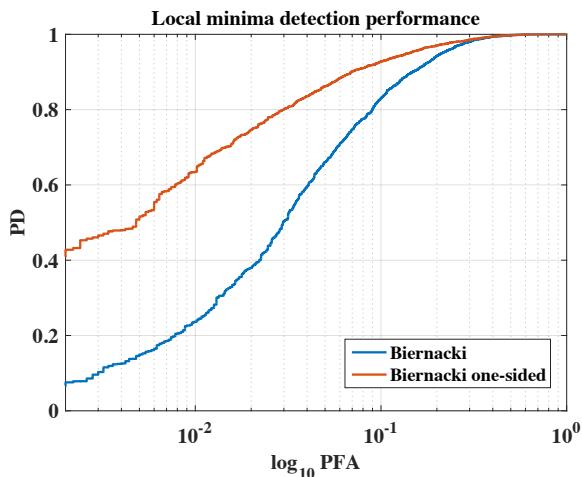


Fig. 2: Detection performance of Biernacki’s two-sided test of a local minimum compared with the one-sided variant for the example problem described by (4)-(6). In this example, the data distribution is in the generalized location family, and Thm. 1 applies, leading to significantly improved performance for the one-sided test.

3.3 Reparameterized Embeddings

Consider a generalized version of the inverse problem (12) with forward model

$$\mathbf{D}_k = \boldsymbol{\mu}(\boldsymbol{\theta}) + \boldsymbol{\varepsilon}_k, \quad k = 1, \dots, n$$

where $\boldsymbol{\mu}(\boldsymbol{\theta}) = \mathbb{E}_{\boldsymbol{\theta}}[\mathbf{D}_k]$, and $\boldsymbol{\varepsilon}_k$ is zero-mean noise whose distribution may depend on $\boldsymbol{\theta}$. We write the log-likelihood as $\ell(\mathbf{d}, \boldsymbol{\mu}(\boldsymbol{\theta}))$ to emphasize its dependence on the mean of the sample \mathbf{D}_k parameterized by $\boldsymbol{\theta}$. Consider the higher dimensional parameterization $\tilde{\boldsymbol{\theta}} = (\boldsymbol{\theta}, \boldsymbol{\theta}') \in \tilde{\boldsymbol{\Theta}}$, $\boldsymbol{\theta} \in \boldsymbol{\Theta}$, $\boldsymbol{\theta}' \in \boldsymbol{\Theta}'$ describing the relaxed mean $\tilde{\boldsymbol{\mu}}(\tilde{\boldsymbol{\theta}})$ that satisfies the property $\tilde{\boldsymbol{\mu}}((\boldsymbol{\theta}, \mathbf{0})) = \boldsymbol{\mu}(\boldsymbol{\theta})$. Let \mathcal{U} and $\tilde{\mathcal{U}}$ represent the range-space of $\boldsymbol{\mu}$ and $\tilde{\boldsymbol{\mu}}$ respectively, and assume that both $\tilde{\boldsymbol{\mu}}$ is continuously differentiable in $\tilde{\boldsymbol{\theta}}$. This reparameterization is defined to be an embedding in the sense that $\mathcal{U} \subseteq \tilde{\mathcal{U}}$, and is a relaxation because the embedding directly implies that

$$\min_{\tilde{\boldsymbol{\theta}} \in \tilde{\boldsymbol{\Theta}}} \{-\ell(\mathbf{d}, \tilde{\boldsymbol{\mu}}(\tilde{\boldsymbol{\theta}}))\} \leq \min_{\boldsymbol{\theta} \in \boldsymbol{\Theta}} \{-\ell(\mathbf{d}, \boldsymbol{\mu}(\boldsymbol{\theta}))\}. \quad (18)$$

More generally, the embedding implies a relaxation in the neighborhood of *all* local minima. Let $\hat{\boldsymbol{\theta}}$ be a local minimum of $-\ell(\mathbf{d}, \boldsymbol{\mu}(\boldsymbol{\theta}))$, and let $S(\hat{\boldsymbol{\theta}}) \subseteq \tilde{\mathcal{U}}$ be the largest path-connected set containing $\boldsymbol{\mu}(\hat{\boldsymbol{\theta}})$ such that $\forall \mathbf{s} \in S$, $-\ell(\mathbf{d}, \mathbf{s}) \leq -\ell(\mathbf{d}, \boldsymbol{\mu}(\hat{\boldsymbol{\theta}}))$. Then the set S contains all path-connected points in $\tilde{\mathcal{U}}$ that improve upon ℓ in the neighborhood of $\hat{\boldsymbol{\theta}}$, and we will refer to a minimizer within this set as $\hat{\tilde{\boldsymbol{\theta}}}$. $\hat{\tilde{\boldsymbol{\theta}}}$ is clearly a function of $\hat{\boldsymbol{\theta}}$ since it is a minimizer over the restricted set $S(\hat{\boldsymbol{\theta}})$, however, this dependency is suppressed in the notation to aid readability. Similarly, let $\tilde{\boldsymbol{\theta}}_0$ represent a point in the relaxed space such that $\tilde{\boldsymbol{\mu}}(\tilde{\boldsymbol{\theta}}_0) = \boldsymbol{\mu}(\boldsymbol{\theta}_0)$. It is helpful to think of $\hat{\tilde{\boldsymbol{\theta}}}$ and $\tilde{\boldsymbol{\theta}}_0$ as unique, however, the ideas presented here can be modified to accommodate a more general case. The key idea behind using a reparameterized embedding to test for consistency of a root of the log-likelihood is to monitor the gap

$$g(\mathbf{d}, \hat{\tilde{\boldsymbol{\theta}}}) = \ell(\mathbf{d}, \tilde{\boldsymbol{\mu}}(\hat{\tilde{\boldsymbol{\theta}}})) - \ell(\mathbf{d}, \boldsymbol{\mu}(\hat{\boldsymbol{\theta}})), \quad (19)$$

and exploit distributional differences in this quantity to test for $H_0 : \hat{\boldsymbol{\theta}} = \hat{\boldsymbol{\theta}}_0$ vs. $H_1 : \hat{\boldsymbol{\theta}} \neq \hat{\boldsymbol{\theta}}_0$. $\hat{\boldsymbol{\theta}}_0$ is the maximizer of the likelihood within the basin of attraction of the true solution $\boldsymbol{\theta}_0$. Notice that (19) takes the form of a generalized likelihood-ratio test between the original parameterization and its relaxation.

Figure 3 illustrates this relaxation when viewed relative to the mean of the measurements. For a relaxation that introduces only a few additional statistical degrees of freedom, one expects the relaxation to only permit a small improvement in the neighborhood of the true solution. Assuming that the Fisher information at $\tilde{\boldsymbol{\theta}}_0$ both exists and is invertible, the asymptotic unbiasedness of the MLE, in conjunction with the fact that the Fisher information increases proportionally to the number of independent observations, ensures that in the neighborhood

of the true solution $E_{\theta_0}[\mu(\hat{\theta}_0)] = E_{\theta_0}[\tilde{\mu}(\hat{\theta}_0)] = \mu(\theta_0)$ [22]. By contrast, no such properties can be ensured in the neighborhoods of the local minima. Indeed, the main motivation for using our embedding relaxation is to alter the local minima structure to emphasize their differences from the global maximum that is close to θ_0 .

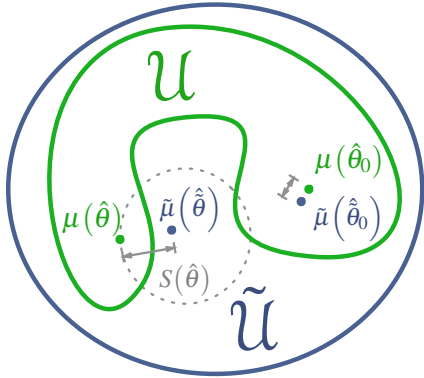


Fig. 3: The reparameterized embedding leads to a relaxation that permits the ML estimator $\hat{\theta}$ to improve within the set $S(\hat{\theta})$. The test for global convergence exploits the distribution differences in the log-likelihood gap between $H_0 : \hat{\theta} = \hat{\theta}_0$ and $H_1 : \hat{\theta} \neq \hat{\theta}_0$.

Figure 4 illustrates the relaxation when viewed relative to the log-likelihood function's value. The solid green line shows the expectation of the negative log-likelihood after relaxation, where this functional is shown on the same domain as the first two functionals by taking a minimum over the compliment of \mathcal{U} relative to $\tilde{\mathcal{U}}$. Given a relaxed parameterization space $\tilde{\Theta}$, the parametric bootstrap of Biernacki can be used to assess the significance of the observed gap. This immediately suggests a test analogous to (11)

$$\frac{g(\mathbf{d}, \hat{\theta}) - m_g(\hat{\theta}, \hat{\theta})}{\sqrt{v_g(\hat{\theta})}} \underset{H_0}{\overset{H_1}{\gtrless}} \tau. \quad (20)$$

where $m_g(\theta, \tilde{\theta}) = E_{\theta}[g(\mathbf{D}, \tilde{\theta})]$ and $v_g(\theta) = \text{Var}_{\theta}[g(\mathbf{D}, \theta)]$.

We now return to the simple example from Section 3.1, with the notation modified slightly to better conform to the discussion on reparameterized embeddings.

$$\hat{\theta}_0 \stackrel{\text{def}}{=} \arg \min_{\theta} \|\mu(\theta) - \mathbf{d}\|^2 \quad \text{s.t.} \quad (21)$$

$$\mu(\theta) = \sin(\theta \mathbf{x}), \quad w \in [0, 4\pi]. \quad (22)$$

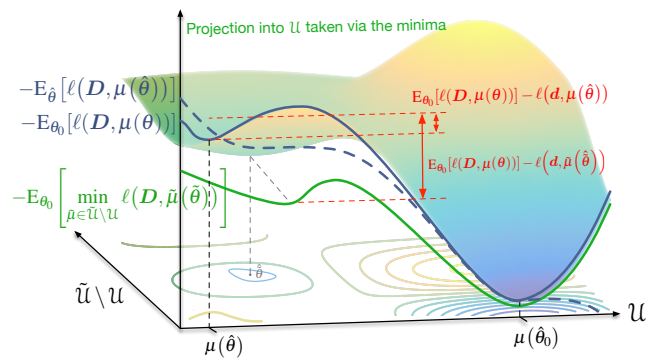


Fig. 4: Diagram illustrating how a locally, but not globally, optimal solution $\hat{\theta}$ can be identified by relaxing the parameter space from Θ to $\tilde{\Theta}$. Under H_1 , minimizing the negative log-likelihood under the relaxation often leads to a relaxed solution $\hat{\theta}$ with a substantially larger gap between its log-likelihood value and the bootstrap estimate (shown in red).

Before discussing how one might identify good reparameterizations, first consider the naive choice of $\tilde{\mu}(\tilde{\theta}) = \sin(\tilde{\theta}_0 \mathbf{x} + \tilde{\theta}_1 \mathbf{x}^2 + \dots + \tilde{\theta}_k \mathbf{x}^{k+1})$. This reparameterization permits spatial variation in the instantaneous frequency while implicitly assuming the phase is known. Figure 5 compares detection performance between Biernacki's test and that given by (20) when the embedding contains one and three additional degrees of freedom ($k = 1$ and $k = 3$ respectively). This illustrates the potential of the proposed approach, however, many problems do not present themselves with an obvious choice of reparameterization.

3.4 Identifying Good Reparameterizations

The use of reparameterized embeddings to test for global convergence is based on the idea one can choose a relaxation such that the log-likelihood function disproportionately benefits under the alternative hypothesis. One is then naturally interested in the marginal cost of the constraints imposed by the parameterization because if these costs were known, the directions leading to the greatest marginal benefit conditioned upon the alternative hypothesis would provide a reasonable basis of relaxation. The remainder of this section describes a practical approach for using a forward model to identify such a basis, and the efficacy of the resulting relaxation is illustrated using our simple example.

Rao was interested in the locally most powerful test for detecting $H_0 : \theta = \theta_0$ against $H_1 : \theta = \theta_0 + \delta$. Rao first considered the case where δ was known. Under this condition, the proportional change in the log-likelihood

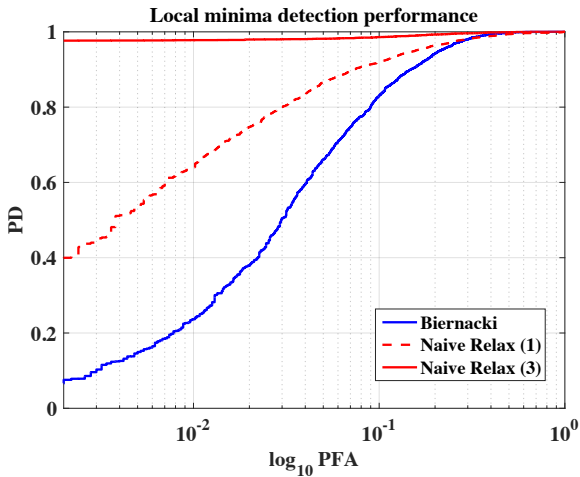


Fig. 5: ROC curve illustrating the potential of reparameterized embeddings when applied to our simple example. The performance of Biernacki’s test is compared with the proposed approach when the naively chosen relaxation has 1 and 3 additional degrees of freedom respectively.

function when moving from θ_0 to $\theta_0 + \delta$ is given by $\delta^T \nabla_{\theta} \ell(\theta_0) = \delta^T \mathbf{s}(\mathbf{d}, \theta_0)$. This results in the test statistic

$$\xi(\delta) = \frac{[\delta^T \mathbf{s}(\mathbf{d}, \theta_0)]^2}{\delta^T \mathbf{I}(\theta_0) \delta}, \quad (23)$$

where $\mathbf{I}(\theta_0)$ is the Fisher information matrix. When δ is unknown, Rao proposed choosing δ to maximize (23). The resulting test is given by

$$\max_{\delta} \xi(\delta) = \mathbf{s}(\mathbf{d}, \theta_0)^T \mathbf{I}(\theta_0)^{-1} \mathbf{s}(\mathbf{d}, \theta_0). \quad (24)$$

Rao’s score test for ML estimators immediately suggests an approach for choosing relaxed parameterizations. Given a set of nominal conditions $\Theta_0 \subseteq \Theta$, for each $\theta_0 \in \Theta_0$ there possibly exists a non-empty set of local minima $L(\theta_0)$ that are stationary points of the ambiguity function which are not equal to θ_0 . Our goal is to identify relaxed parameterizations that maximally discriminate between $H_0 : \theta = \theta_0$ and $H_1 : \theta \in L(\theta_0)$.

Consider a greatly relaxed reparameterized embedding $\tilde{\Theta}$, say the measurement domain. As before, let $\tilde{\theta}_0$ represent a point in the relaxed space such that $\tilde{\mu}(\tilde{\theta}_0) = \mu(\theta_0)$, and let $\tilde{\mathbf{I}}(\tilde{\theta}_0)$, and $\tilde{\mathbf{s}}(\tilde{\theta}_0)$, represent the Fisher information matrix and the score evaluated at the restricted ML estimate respectively. For each local minima encountered, the score function in the relaxed space identifies the direction of greatest improvement of the log-likelihood had all of the additional degrees of freedom of the relaxed parameterization been available. Using a collection of these points, one can identify the

single additional degree of freedom that maximally distinguishes between the encountered members in $L(\theta_0)$ and θ_0 . The proposed procedure for identifying candidate relaxation dimensions is described by Algorithm 1. If more than one additional relaxation dimension is desired, this procedure can be repeated with previously identified dimensions removed from the relaxed space, and included in the restricted estimator.

Input: Θ_0 : Set of nominal true parameters
Input: Θ_s : Set of starting points
Input: $\tilde{\Theta}$: Space of the relaxed embedding
Output: r : Relaxation dimension

- 1 **for** $(\theta_0^{(i)}, \theta_s^{(i)}) \in \Theta_0 \times \Theta_s$ **do**
- 2 Generate noise-free data $d_{n,f}$
- 3 Solve for the restricted ML estimator $\hat{\theta}(d_{n,f})$
 from $\theta_s^{(i)}$
- 4 **if** $\hat{\theta} \neq \theta_0^{(i)}$ **then**
- 5 Record the whitened score vector:
 $[\Delta]_{:,j} = \tilde{\mathbf{I}}(\tilde{\theta}_0^{(i)})^{-1/2} \tilde{\mathbf{s}}(\mathbf{d}, \hat{\theta})$
- 6 $r = \mathbf{u}^{(1)} \stackrel{\text{def}}{=} \text{First left-singular vector of } \Delta$

Algorithm 1: Algorithm for identifying relaxation.

To demonstrate the efficacy of the proposed approach, once again consider our simple example of detecting convergence to a local minimum when estimating the frequency of a sinusoid in noise (21)-(22). The algorithm described in Figure 1 was run with the nominal conditions Θ_0 chosen to be 100 equally spaced frequencies over the interval $[0, 4\pi]$, and the relaxed embedding $\tilde{\Theta}$ chosen to be the entire measurement domain $\tilde{\mu}(\tilde{\theta}) \in \mathcal{R}^{100}$. Figure 6 shows the additional relaxation direction \mathbf{r} suggested by the proposed procedure. Using this additional degree of freedom, the relaxed embedding used in conjunction with the test given by (20) becomes $\tilde{\mu}(\tilde{\theta}) = \sin([\tilde{\theta}]_1 \mathbf{x}) + [\tilde{\theta}]_2 \mathbf{r}$. Figure 7 shows how the relaxed embedding alters the structure of the expected minima of the negative log-likelihood and increases the gap (19). This figure is analogous to the conceptual diagram shown in Figure 4, and the ROC curve associated with the resulting test shown in Figure 8.

4 Application to Wavefront Sensing

In [21], the authors present a joint ML approach for the simultaneous estimation of camera-blur and pose from a known calibration target in the presence of aliasing. The Cramér-Rao Bound (CRB) for this problem is derived, and simulations demonstrate that the proposed estima-

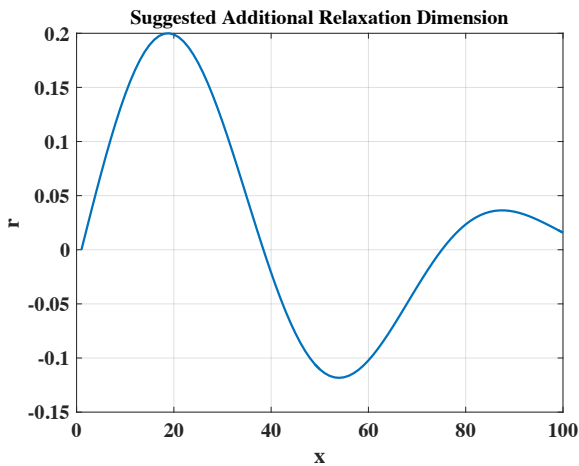


Fig. 6: Additional relaxation dimension suggested by the procedure given in Figure 1.

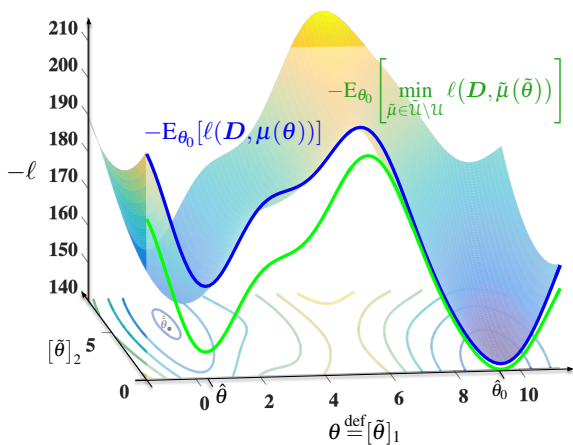


Fig. 7: Expected negative log-likelihood associated with the simple example given by (21)-(22) under the 1-dimensional relaxation provided by the algorithm described in Algorithm 1. This figure is analogous to the conceptual plot shown in Algorithm 4, and illustrates how a well-chosen relaxed embedding can be used to detect convergence to local minima.

tor achieves near-optimal MSE performance when the global maxima of the likelihood can be located. The PSF is described using a Zernike basis representation [40] of the phase-aberrations in the exit pupil of an otherwise ideal imaging system. This blur description parsimoniously represents common manufacturing errors [32]. Unfortunately, it also results in a highly non-convex log-likelihood with many spurious roots. Under moderate levels of blur and high SNR conditions gradient-descent starting from an ideal imaging system led to a local minimum 96% of the time [21]. Each of the aforementioned tests for convergence to a local minimum was used to evaluate the resulting set of stationary points; however,

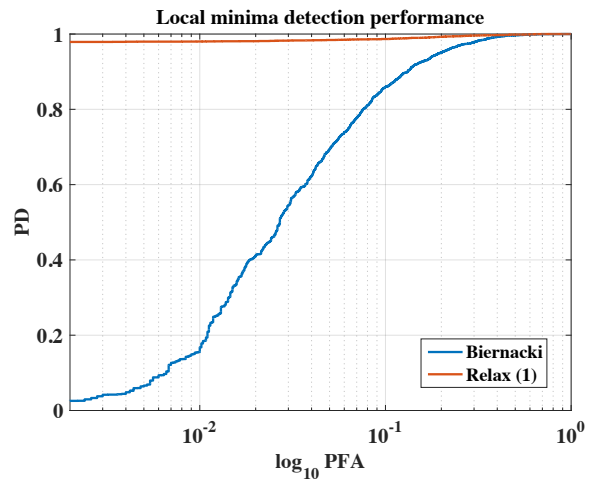


Fig. 8: ROC curve comparing Biernacki's test to the reparameterized embedding approach when using a single relaxation dimension suggested by the procedure described in Algorithm 1

none were found not to be reliable. Consistent with the earlier findings of Blatt and Hero, Biernacki's test performed best, but with a type-1 error rate of $\alpha = 0.01$ still only detected 21 of the 96 local minima's encountered ($\beta = 0.22$). Such a low probability of detection would be undesirable in most applications.

Using the technique described in Section 3.3, with the relaxation basis given by the space of non-negative PSFs on a diffraction-limited grid, the proposed technique rejected all 100 of the local minima at a type-1 error rate of $\alpha = 0.01$. By combining this test with a strategy for restarting the algorithm when a local minimum is detected, the author's were able to construct an application-specific search strategy that substantially outperformed generic simulated annealing.

After one detects convergence to a local minimum, it is preferable to use a search restart-procedure that takes into account information contained in the location of the current stationary point. The proposed restart mechanism is also application specific, and exploits the structure of a wavefront description of the PSF to identify alternative wavefront solutions that are also probable minima. Consider the PSF h corresponding to the perturbed phase-screen $\Psi + \beta$. One may write the PSF as [17]

$$h = c_0 |\mathcal{F}^{-1}\{Ae^{j\Psi} A_B e^{j\beta}\}|^2 \quad (25)$$

$$= c_0 |\mathcal{F}^{-1}\{Ae^{j\Psi}\} * \mathcal{F}^{-1}\{A_B e^{j\beta}\}|^2 \quad (26)$$

$$= c_0 |g * d|^2, \quad (27)$$

where \mathcal{F}^{-1} is the inverse Fourier transform, $A_B = 1_{\text{supp}(A)}$ is the binary aperture corresponding to the support of A , g and d are the coherent PSF's corresponding

to the unperturbed PSF and the perturbing phase-screen respectively, and c_0 is a constant that causes the PSF to integrate to 1. Letting δ be the Kronecker delta function, and a an arbitrary complex constant such that $|a| = 1$, the $(m, n)^{\text{th}}$ element of the discrete representation of h is given by

$$[h]_{m,n} = c_0 |\langle g(m-x, n-y), d \rangle|^2 \quad (28)$$

$$= c_0 |\langle g(m-x, n-y), a\delta + (d - a\delta) \rangle|^2 \quad (29)$$

$$= c_0 \left[| [g]_{m,n} |^2 + |\langle g(m-x, n-y), d - a\delta \rangle|^2 \right] + 2\Re(a [g]_{m,n}^H \langle g(m-x, n-y), d - a\delta \rangle). \quad (30)$$

The magnitude of the PSF change induced by β at the $(m, n)^{\text{th}}$ element is then given by

$$|[\epsilon]_{m,n}| = \left| [h]_{m,n} - c_0 |[g]_{m,n}|^2 \right| \quad (31)$$

$$= c_0 \left| |\langle g(m-x, n-y), d - a\delta \rangle|^2 + \right. \quad (32)$$

$$\left. 2\Re(a [g]_{m,n}^H \langle g(m-x, n-y), d - a\delta \rangle) \right| \leq c_0 \left| |\langle g(m-x, n-y), d - a\delta \rangle|^2 + \right. \quad (33)$$

$$\left. 2|[g]_{m,n}| |\langle g(m-x, n-y), d - a\delta \rangle| \right| \quad (34)$$

$$\leq c_0 \left[\|g\|^2 \|d - a\delta\|^2 + 2|[g]_{m,n}| \|g\| \|d - a\delta\| \right] \quad (35)$$

$$\leq \|d - a\delta\| \left[\|d - a\delta\| + 2 \frac{|[g]_{m,n}|}{\|g\|} \right]. \quad (36)$$

This point-wise bound on the PSF perturbation ϵ , associated with the wavefront perturbation β , is clearly minimized when $\angle a = \angle [d]_{0,0}$. Under this condition, the right-hand side of (36) is monotonic in the Strehl ratio [23] associated with β , which we will denote as $c_0 |[d]_{0,0}(\beta)|^2$. Thus, the set of wavefronts that maximize the Strehl ratio for a fixed RMS strength also minimize the worst-case, point-wise error in the perturbed PSF. These wavefronts are given by

$$\left\{ \beta = \arg \max_{\tilde{\beta}} \tilde{\beta} c_0 |[d]_{0,0}(\tilde{\beta})|^2 : \|\tilde{\beta}\|^2 = \tau \right\}. \quad (37)$$

Determining this set is related to the problem of wavefront balancing, and it is well known that such sets are generally discontinuous in aberration space, and have no closed form solution [23]. Fortunately, this set is independent of locally optimal phase screen Ψ , and thus once computed may be reused for other problems. We have identified this set of points numerically under a basis containing the first 12 Zernike modes for perturbations up to 0.2 waves RMS. Figure 9 shows a 2D embedding

of the points given by (37) for RMS perturbations up to 0.09 waves, and Figure 10 shows a PSF corresponding to a phase-screen of 0.25 waves RMS as well as the first few perturbations drawn from the set given for $\tau = 0.2$. This latter plot clearly suggests the utility of this class of perturbations for reinitializing a global search strategy.

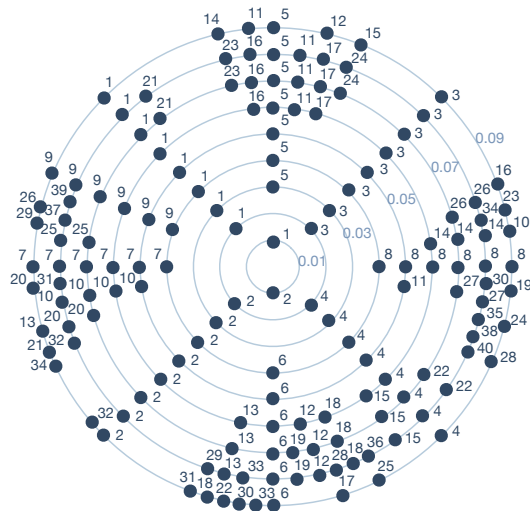


Fig. 9: A 2D embedding of the points within the space of the first 12 Zernike modes that maximize the Strehl ratio for shells of a fixed RMS wavefront deviation. Shells up to 0.09 waves RMS are shown, with the points numbered to indicate correspondence between phase-screens in neighboring shells. Note that the asymmetries are not unusual when embedding high-dimensional surfaces into 2D.

A Monte Carlo simulation was performed to assess the efficacy of the proposed approach for identifying the MLE of the optical inverse-problem investigated in [21]. The simulated imaging system was configured to provide reasonably high output SNR of 100 (c.f. [21] Section 4), and the number of aberration parameters varied to alter the problem difficulty. As the number of Zernike modes in the model increases, so too does the probability of encountering local minima, and thus overall search times increase. The number of consecutive Noll-ordered Zernike modes [30] was varied from 1 (defocus only) to 12 (all wavefront modes of radial orders 2 through 4). A limited-memory quasi-Newton search was used to identify stationary points of the log-likelihood starting from a diffraction-limited model. If the reparameterized embedding approach described in Section 3.3 failed to reject the null hypothesis at a power level of $\alpha = 0.01$ the search was terminated, otherwise a new starting point 0.2 waves RMS away from the current minimum was chosen according to (37), and the search was con-

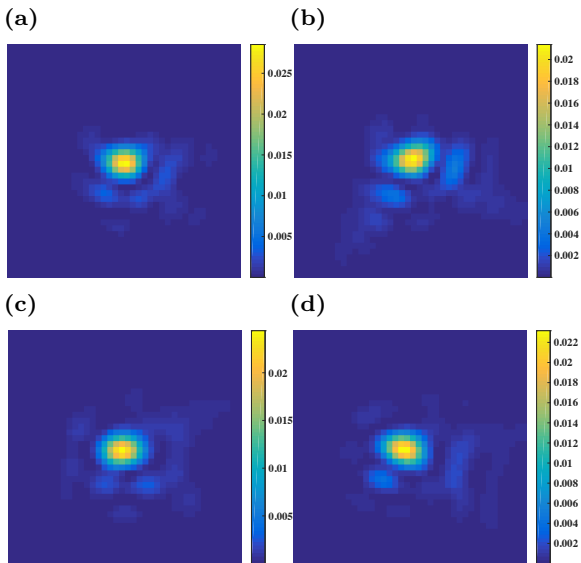


Fig. 10: A PSF corresponding to a random phase-aberration of 0.25 waves RMS is shown in (a). (b)–(d) show the first few perturbations of 0.2 waves RMS drawn from the set given by (37). Each of the PSF’s are displayed at 2X the Nyquist rate for the optical system.

tinued. The ability of the proposed application-specific optimization strategy to terminate as soon as a likely global optimum is detected leads to substantial runtime improvements.

The proposed approach for constructing tests for convergence to local minima of the log-likelihood function, in conjunction with an application-specific restart strategy, led to a practical approach for solving this inverse problem. Figure 11 shows the mean and standard errors of runtimes corresponding to 10 independent realizations of the same camera model. The simulated annealing algorithm provided in MATLAB[®] Optimization Toolbox version 8.0 was used as a point of reference, where this algorithm was provided objective function gradients and stopped the first time *any test point fell within 0.01 waves RMS of the true solution*. In the astronomical imaging community wavefront descriptions of optical systems typically include Zernike models up to at least radial-order 3 (7 Zernike modes). For models of this complexity, the proposed global optimization strategy results in 5X improvement in total runtime over the simulated annealing algorithm that was prematurely stopped after any test point fell within 0.01 waves RMS of the global minimum. When the same annealing algorithm is permitted to run until convergence, the proposed approach is around 2 orders of magnitude faster.

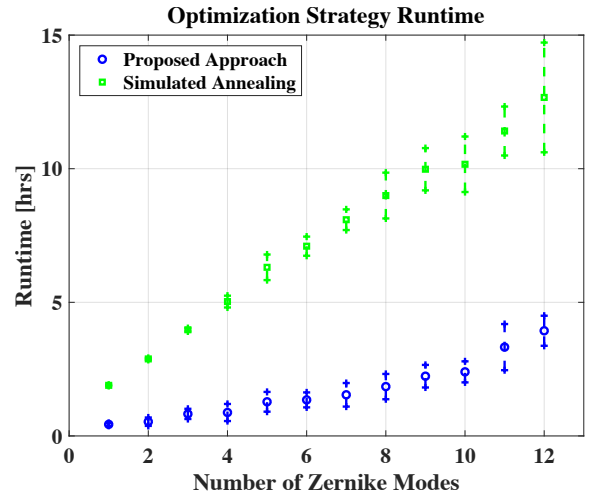


Fig. 11: Monte-Carlo study of optimization runtimes as a function of the number of aberration modes in the model.

5 Concluding Remarks

Mila Nikolova was keenly aware of the vital role that implicitly defined estimators play in inverse-imaging. When the objective function of interest is non-convex, and the dimension of the problem reasonably large, general-purpose global optimization techniques are often impractical. In such cases, tests for convergence to sub-optimal solutions serve an important role. This paper presents an improved one-sided test for detecting convergence to local minima when the imaging model results in distributions from the generalized location family. Under this assumption, we demonstrate that the global minima validation function proposed by Biernacki [7] is always negative in expectation, and use this result to construct an improved test for this class of problems. We also introduce a new test based on reparameterized embeddings and show how to construct problem-specific tests when one has access to a generative forward model. These ideas are illustrated using a simple example, and code for reproducing the key figures from this document is available at <https://github.com/jwleblan/localMinima>. Finally, the applicability of the proposed approach to complex inverse-imaging problems is demonstrated in the context of camera blur recovery [21]. While we believe these new tools will find many applications in the imaging community, the design of optimal tests for convergence to global rather than local optimum remains an important open question.

Acknowledgements This work was partially supported by ARO grant W911NF-15-1-0479 and a DOE NNSA grant to the University of Michigan Consortium on Verification Technology.

References

1. Aitchison, J., Silvey, S.: Maximum-likelihood estimation of parameters subject to restraints. *The Annals of Mathematical Statistics* pp. 813–828 (1958)
2. Aitchison, J., Silvey, S.D.: Maximum-likelihood estimation procedures and associated tests of significance. *Journal of the Royal Statistical Society. Series B (Methodological)* pp. 154–171 (1960)
3. Alberge, F., Nikolova, M., Duhamel, P.: Blind identification/equalization using deterministic maximum likelihood and a partial prior on the input. *IEEE transactions on signal processing* **54**(2), 724–737 (2006)
4. Andrieu, C., Doucet, A.: Simulated annealing for maximum a posteriori parameter estimation of hidden markov models. *Information Theory, IEEE Transactions on* **46**(3), 994–1004 (2000)
5. Andrieu, C., Doucet, A., Fitzgerald, W.J.: An introduction to monte carlo methods for bayesian data analysis. In: *Nonlinear Dynamics and Statistics*, pp. 169–217. Springer (2001)
6. Bertsekas, D.P.: *Nonlinear programming*. Athena Scientific (1999)
7. Biernacki, C.: Testing for a global maximum of the likelihood. *Journal of Computational and Graphical Statistics* **14**(3), 657–674 (2005)
8. Blatt, D., Hero, A.O.: On tests for global maximum of the log-likelihood function. *Information Theory, IEEE Transactions on* **53**(7), 2510–2525 (2007)
9. Cox, D., Hinkley, D.: *Theoretical Statistics*. Chapman and Hall, London (1974)
10. Cox, D.R.: Tests of separate families of hypotheses. In: *Proceedings of the fourth Berkeley symposium on mathematical statistics and probability*, vol. 1, pp. 105–123 (1961)
11. Cox, D.R.: Further results on tests of separate families of hypotheses. *Journal of the Royal Statistical Society: Series B (Methodological)* **24**(2), 406–424 (1962)
12. Cramér, H.: *Mathematical methods of statistics*. Princeton university press (1946)
13. Durand, S., Nikolova, M.: Stability of the minimizers of least squares with a non-convex regularization. part i: Local behavior. *Applied Mathematics and Optimization* **53**(2), 185–208 (2006)
14. Durand, S., Nikolova, M.: Stability of the minimizers of least squares with a non-convex regularization. part ii: Global behavior. *Applied Mathematics and Optimization* **53**(3), 259–277 (2006)
15. Fisher, R.A.: Theory of statistical estimation. In: *Mathematical Proceedings of the Cambridge Philosophical Society*, vol. 22, pp. 700–725. Cambridge University Press (1925)
16. Gan, L., Jiang, J.: A test for global maximum. *Journal of the American Statistical Association* **94**(447), 847–854 (1999)
17. Goodman, S.N.: Toward evidence-based medical statistics: The p value fallacy. *Annals of Internal Medicine* **130**(12), 995–1004 (1999)
18. Kotz, S., Balakrishnan, N., Johnson, N.L.: *Continuous multivariate distributions, Volume 1: Models and applications*, vol. 1. John Wiley & Sons (2004)
19. Kullback, S.: *Information theory and statistics*. Courier Corporation (1997)
20. Le Cam, L.: *Asymptotic methods in statistical decision theory*. Springer Science & Business Media (2012)
21. LeBlanc, J.W., Thelen, B.J., Hero, A.O.: Joint camera blur and pose estimation from aliased data. *J. Opt. Soc. Am. A* **35**(4), 639–651 (2018)
22. Lehmann, E., Casella, G.: *Theory of Point Estimation*. Springer (1998)
23. Martial, G.: Strehl ratio and aberration balancing. *J. Opt. Soc. Am. A, Opt. Image Sci. (USA)* **8**(1), 164 – 70 (1991)
24. Nikolova, M.: Estimées localement fortement homogenes. *Comptes Rendus de l’Académie des Sciences-Series I-Mathematics* **325**(6), 665–670 (1997)
25. Nikolova, M.: Markovian reconstruction using a gnc approach. *IEEE Transactions on Image Processing* **8**(9), 1204–1220 (1999)
26. Nikolova, M.: Model distortions in bayesian map reconstruction. *Inverse Problems and Imaging* **1**(2), 399 (2007)
27. Nikolova, M., Hero, A.: Segmentation of a road from a vehicle-mounted radar and accuracy of the estimation. In: *Proceedings of the IEEE Intelligent Vehicles Symposium 2000 (Cat. No. 00TH8511)*, pp. 284–289. IEEE (2000)
28. Nikolova, M., Idier, J., Mohammad-Djafari, A.: Inversion of large-support ill-posed linear operators using a piecewise gaussian mrf. *IEEE Transactions on Image Processing* **7**(4), 571–585 (1998)
29. Nocedal, J., Wright, S.: *Numerical Optimization*. Springer (1999)
30. Noll, R.J.: Zernike polynomials and atmospheric turbulence. *J. Opt. Soc. Am.* **66**(3), 207–211 (1976)
31. Rao, R.C.: Large sample tests of statistical hypotheses concerning several parameters with applications to problems of estimation. In: *Mathematical Proceedings of the Cambridge Philosophical Society*, vol. 44, pp. 50–57. Cambridge Univ Press (1948)
32. Shannon, R., Wyant, J.: *Applied Optics and Optical Engineering*, vol. XI. Academic Press (1992)
33. Sharman, K., McClurkin, G.: Genetic algorithms for maximum likelihood parameter estimation. In: *IEEE International Conference on Acoustics, Speech and Signal Processing*, pp. 2716 – 19. New York, NY, USA (1989)
34. Silvey, S.D.: The lagrangian multiplier test. *Ann. Math. Statist.* **30**(2), 389–407 (1959)
35. Stigler, S.M., et al.: The epic story of maximum likelihood. *Statistical Science* **22**(4), 598–620 (2007)
36. Wald, A.: Tests of statistical hypotheses concerning several parameters when the number of observations is large. *Transactions of the American Mathematical society* **54**(3), 426–482 (1943)
37. Wald, A.: Note on the consistency of the maximum likelihood estimate. *The Annals of Mathematical Statistics* **20**(4), 595–601 (1949)
38. White, H.: Maximum likelihood estimation of misspecified models. *Econometrica: Journal of the Econometric Society* pp. 1–25 (1982)
39. Wilks, S.S.: The large-sample distribution of the likelihood ratio for testing composite hypotheses. *Ann. Math. Statist.* **9**(1), 60–62 (1938)
40. Zernike, v.F.: Beugungstheorie des schneidener-fahrens und seiner verbesserten form, der phasenkontrastmethode. *Physica* **1**(7), 689–704 (1934)